Virchows Archiv A Pathol Anat (1991) 418:185–192

Virchows Archiv A
Pathological Anatomy and Histopathology

Three-dimensional ultrastructure of glomerular injury in serum sickness nephritis using the quick-freezing and deep-etching method

Atsuhiko Naramoto [1], Shinichi Ohno [2], Koh Nakazawa [1], Hiroya Takami [1], Nubuo Itoh [1], and Hidekazu Shigematsu [1]

Departments of [1] Pathology and [2] Anatomy, Shinshu University School of Medicine, Matsumoto 390, Japan

Received August 29, 1990 / Accepted October 15, 1990

Summary. The three-dimensional ultrastructure of the glomerulus in serum sickness nephritis has been investigated by the quick-freezing and deep-etching method. Compact granular immune deposits were localized in filamentous networks in the lamina densa and mesangial matrices. These constitutional fibrils with diameters of 8–15 nm, were directly attached to the immune deposits. The filamentous networks became markedly loosened around the deposits. In podocytes, reticular microfilaments with positive decoration by myosin subfragment 1 (S1) were increased in flattened foot processes and directly attached to the cell membranes. Fine filaments with diameters of 4–7 nm were undecorated by S1 and connected with actin filaments as cross-bridges. Intermediate filaments were also increased in the cell bodies and primary processes of podocytes. Connecting fibrils in lamina rara externa were partially disrupted. The immune deposits were primarily detected in the networks of lamina densa and actually destroyed the size barrier composed of filamentous networks. Moreover, the mesangial deposits also disorganized mesangial networks to probably alter mesangial flow through the matrices. Increased actin filaments in foot processes seemingly reinforced the cell membranes and the connecting fibrils in lamina rara externa, which prevented the initial detachment of podocytes from the basement membrane.

Key words: Serum sickness nephritis – Quick freezing – Deep etching – Immune deposit – Actin filaments

Introduction

The development of glomerulonephritis is mainly based on immunological reactions. Eighty percent of human glomerulonephritis is recognized to be induced by immune complexes (Dixon and Wilson 1976). The category includes immunocomplex glomerulonephritis such as IgA nephropathy, membranous glomerulonephritis, membranoproliferative glomerulonephritis including dense deposit disease and poststreptococcal glomerulonephritis. At least three types of immune mechanisms, anti-glomerular antibody, in situ immune complex formation and circulating immune complexes, participate in the initiation and development of glomerulonephritis. Experimental serum sickness nephritis is a suitable model for immunocomplex glomerulonephritis induced by the circulating immune complexes (Bolton and Sturgill 1978; Shigematsu and Yano 1986; Yamamoto et al. 1978). In this model, however, the three-dimensional relationship of the immune deposits and extracellular matrices of glomerular basement membranes and mesangium has not been analysed. This is important in understanding the initiation and fate of the glomerular tissue injuries.

The quick-freezing and deep-etching method, which is one of the new techniques in the electron microscopic field (Heuser and Kirschner 1980; Kubosawa and Kondo 1985; Ohno 1985; Ohno and Takasu 1989), has the advantage of examining the three-dimensional ultrastructures of tissues in vivo at high resolution. We have already demonstrated the hepatocyte cytoskeletons in various pathological models (Naramoto 1988; Naramoto et al. 1988a, b, 1990; Ohno and Fujii 1990). In the present study, we examined how immune deposits appear in the extracellular matrices of glomerular basement membranes and mesangium. Particular attention is paid to cytoskeletal changes in podocytes.

Offprint requests to: A. Naramoto, First Department of Pathology, Shinshu University School of Medicine, 3-1-1 Asahi, Matsumoto 390, Japan

Materials and methods

Serum sickness nephritis was induced in 30 male Fischer rats (F 344/Du Crj) according to the methods of Yamamoto et al. (1978) and Bolton and Sturgill (1978) with some modifications (Shigematsu and Yono 1986). These rats were given 500 μg egg albumin with an equal volume of Freund's complete adjuvant into the footpads as pre-immunization. After 30 days, each rat was injected

intraperitoneally with increasing amounts of egg albumin for 28 days (1 mg on the 1st day, 2 mg on the 2nd day, 5 mg on the 3rd and 4th days, and 10 mg each for the last 24 days). A control group consisted of 5 untreated rats.

The kidneys from these animals were perfused with 2% paraformaldehyde in 0.1 M phosphate buffer (PB), pH 7.4, via the abdominal aorta for 5 min. The renal cortices were immediately cut into small pieces ($2 \times 2 \times 4$ cm) with razor blades and washed in PB for 30 min to remove the soluble proteins from tissue surfaces. Some of them were incubated in PB containing myosin subfragment 1 (S1, 1 mg/ml) at room temperature for 30 min in order to identify actin filaments near the cut tissue surfaces (Naramoto et al. 1990). The S1-treated or untreated tissues were postfixed with 0.25% glutaraldehyde in PB for 30 min. They were rinsed with 10% methanol and quickly frozen in isopentane-propane mixture (around $-190°$ C) cooled in liquid nitrogen. The tissue surfaces of the frozen specimens were fractured with a scalpel in liquid nitrogen. They were deeply etched in an Eiko FD-3S machine at $-95°$ C, $2–6 \times 10^{-7}$ Torr, for 15–20 min and rotary shadowed with platinum and carbon. The replica membranes with the specimens were taken out and immediately coated with 2% collodion. The kidney tissues were dissolved in sodium hypochlorite. The replica membranes were put on grids and immersed in amylacetate solution to dissolve the collodion. They were observed in a Hitachi HS-9 electron microscope.

For freeze-fracture immunohistochemistry the specimens were fixed with 2.5% glutaraldehyde in PB for 3 h once again and treated with 20% sucrose and 10% glycerol in PB for 2 h. They were quickly frozen in the isopentane-propane mixture cooled in liquid nitrogen. The tissue surfaces of the frozen specimens were fractured with a scalpel in the liquid nitrogen. They were thawed and washed in PB. The tissue surfaces were treated with 0.1 M lysine in PB and incubated with anti-rat IgG for 2 h at room temperature. They were washed in 0.1 M phosphate buffered saline (PBS) and incubated with protein A-gold (20 nm; E-Y Laboratories, San Mateo, Calif., USA) at 4° C for 12 h. They were then treated with 10% methanol and quickly frozen in the isopentane-propane mixture. They were processed for replica preparations as mentioned above.

Small pieces of renal cortices were prefixed with 2.5% glutaraldehyde in PB and postfixed with 1.5% osmium tetroxide in PB. They were dehydrated in a graded series of ethanol and embedded in Quetol 812; ultrathin sections were then cut with diamond knives and were stained with uranyl acetate and lead citrate.

Results

In control rats, networks of the fibrils with diameters of 8–15 nm were noted in the middle layer of the glomerular basement membranes, corresponding to the lamina densa in ultrathin sections (Fig. 1a). The diameters of mesh pores were about 15 nm. Ladder-like connecting fibrils anchored the networks of the lamina densa perpendicularly with the outer surfaces of podocytes or endothelial cells. Paramesangial matrices had looser networks than those of the lamina densa (Fig. 1b). The diameters of such mesh pores ranged from 20 nm to 45 nm. The fibrils with diameters of 8–15 nm were attached directly to mesangial cell membranes. Meshwork-like filaments were also seen in the foot processes of podocytes (Fig. 1).

In the glomeruli of serum sickness nephritis, many hump-like deposits were localized along peripheral basement membranes (Fig. 2a, b). Some of the deposits protruded towards subepithelial portions. Such compact granular deposits were confirmed as immune deposits on replica membranes by freeze-fracture immunohistochemistry with anti-IgG (Fig. 2b, inset). Densely packed microfilaments were increased within the flattened foot processes, which covered the deposits. At higher magnification, deposits were also localized in the lamina densa of peripheral basement membranes (Fig. 2c). Many fibrils organizing the lamina densa were attached to the deposits. The pore sizes of networks of lamina densa became irregularly dilated to 30–60 nm in diameter, around deposits. However, connecting fibrils in lamina rara externa were preserved regularly in these areas. Deposits were also seen in the filamentous network of the mesangial matrix (Fig. 3a). At higher magnification, compact granular deposits were attached to many constituent fibrils in mesangial matrix and mesangial lamina densa (Fig. 3b). The filamentous networks around the deposits were disrupted and dilated up to 50–80 nm in diameter.

S1-decorated filaments with diameters of 15–20 nm were increased in the flattened foot processes of podocytes (Fig. 4a). They were connected with each other and directly attached to the cell membranes beneath the basement membranes. S1-undecorated fine filaments with diameters of 4–7 nm were connected with actin filaments on both ends as cross-linking filaments. Moreover, intermediate filaments were also increased in the primary processes and main cell bodies of podocytes (Fig. 4b).

The detachment of podocytes from the basement membranes was sometimes seen in conventional ultrathin sections (Fig. 5a). Connecting fibrils in lamina rara externa were observed to be disrupted in these areas by the quick-freezing and deep-etching method (Fig. 5b, c).

Discussion

New ultrastructural findings with this technique have been reported one after another in various tissues (Naramoto 1988; Naramoto et al. 1990; Ohno 1985; Ohno and Takasu 1989; Ohno and Fujii 1990) by our group. In the present study, we reveal the in vivo network structures of glomerular basement membranes and mesangial matrices and the cytoskeletons of podocytes. Fibrillar networks are connected to the podocytes, mesangial cells and endothelial cells by ladder-like connecting fibrils, which seemed to be important for the preservation of cell-matrix connection and location.

We described here ultrastructural changes in glomerular basement membranes and mesangial matrices decorated by the deposits. Such compact granular deposits have been confirmed as immune deposits on replica membranes by freeze-fracture immunohistochemistry with anti-egg albumin or anti-IgG. Immune deposits at the initial phase appeared to be trapped within fibrillar networks of lamina densa in the peripheral basement membranes. This is because the connecting fibrils organizing lamina rara externa were preserved without deposition in the areas. We speculate that the deposits grow and translocate towards the subepithelial areas, and finally localize as subepithelial deposits, although to es-

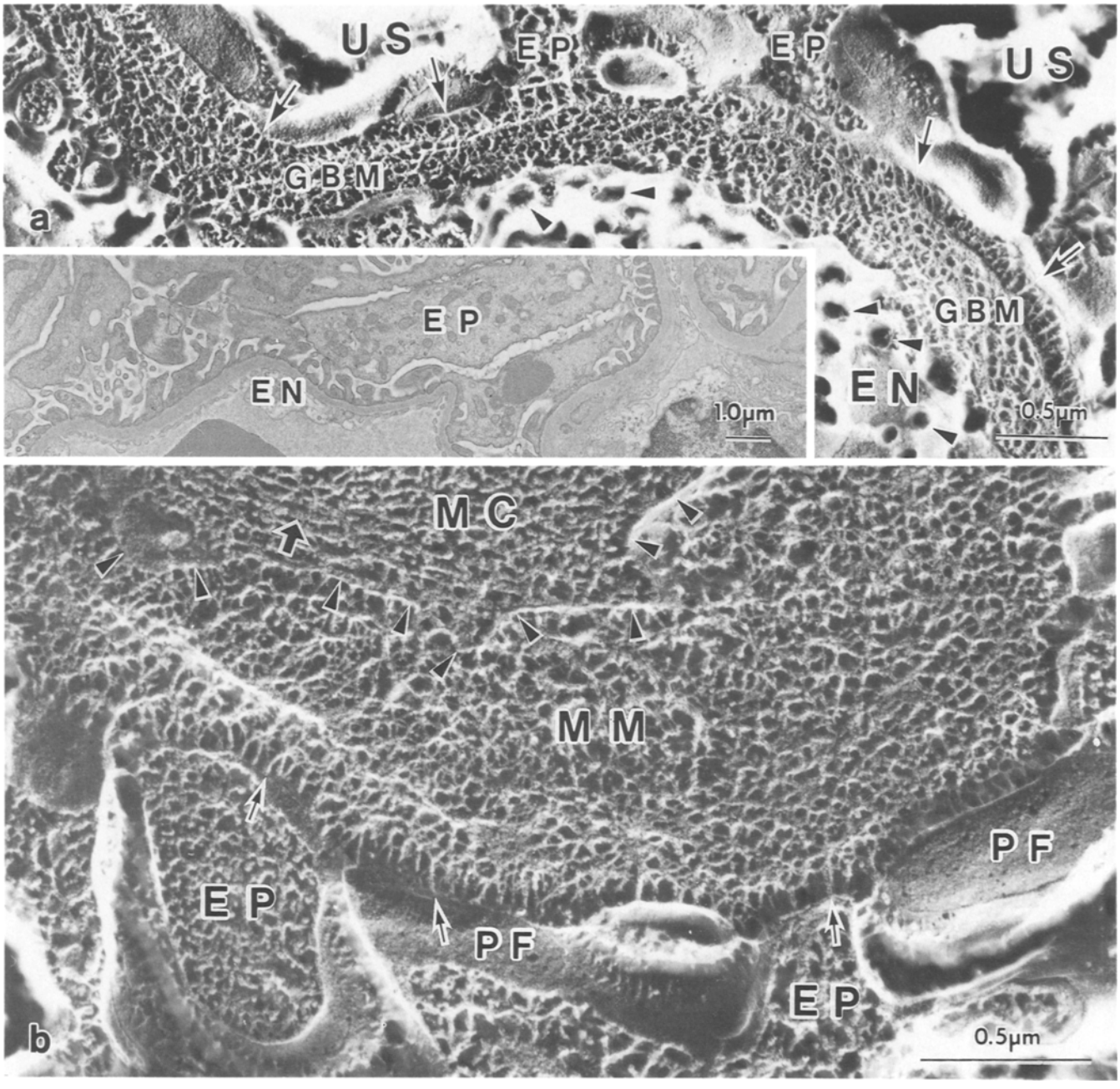

Fig. 1a, b. Replica electron micrographs of control glomeruli. **a** Middle layer of peripheral glomerular basement membrane (*GBM*), corresponding to the lamina densa in ultrathin section, is composed of meshwork architectures of fibrils with diameters of 8–15 nm. Connecting fibrils (*arrows*) in lamina rara externa are directly attached to the cell membranes of podocytes. *EP*, Podocyte; *EN*, endothelial cell with fenestrae (*arrowheads*); *US*, urinary space. ×34800. *Inset*: Corresponding micrograph of conventional ultrathin section. ×7200. **b** Mesangial matrix (*MM*) has looser networks of fibrils than lamina densa. These fibrils are attached to mesangial cells (*MC*). Connecting fibrils in lamina rara externa are attached to the cell membranes of podocytes (*small arrows*). Microfilaments in the foot processes (*EP*) and bundled intermediate filaments (*large arrows*) in the mesangial cell are clearly visible. *Arrowheads* indicate the mesangial cell membrane. *PF*, P face of podocyte. ×54000

tablish this the changes should be examined at different time intervals after the egg albumin treatment. The fibrillar networks of the lamina densa become irregular due to the dilatation of meshes around the immune deposits. It has been recognized that the lamina densa in intact glomeruli has a size barrier which is composed of regular fibrillar networks of type IV collagen (Laurie et al. 1984). Subsequent immune deposition may result in the disruption and disorganization of this barrier and be followed by the development of proteinuria. Kihara et al. (1990) reported that the deposits in the extracellular matrix were positive for antigen, antibody and complement factors, but were negative for type IV collagen, laminin, fibronectin and heparan sulphate proteoglycan in the experimental serum sickness model, using post-embedding immunoelectron microscopy. This observa-

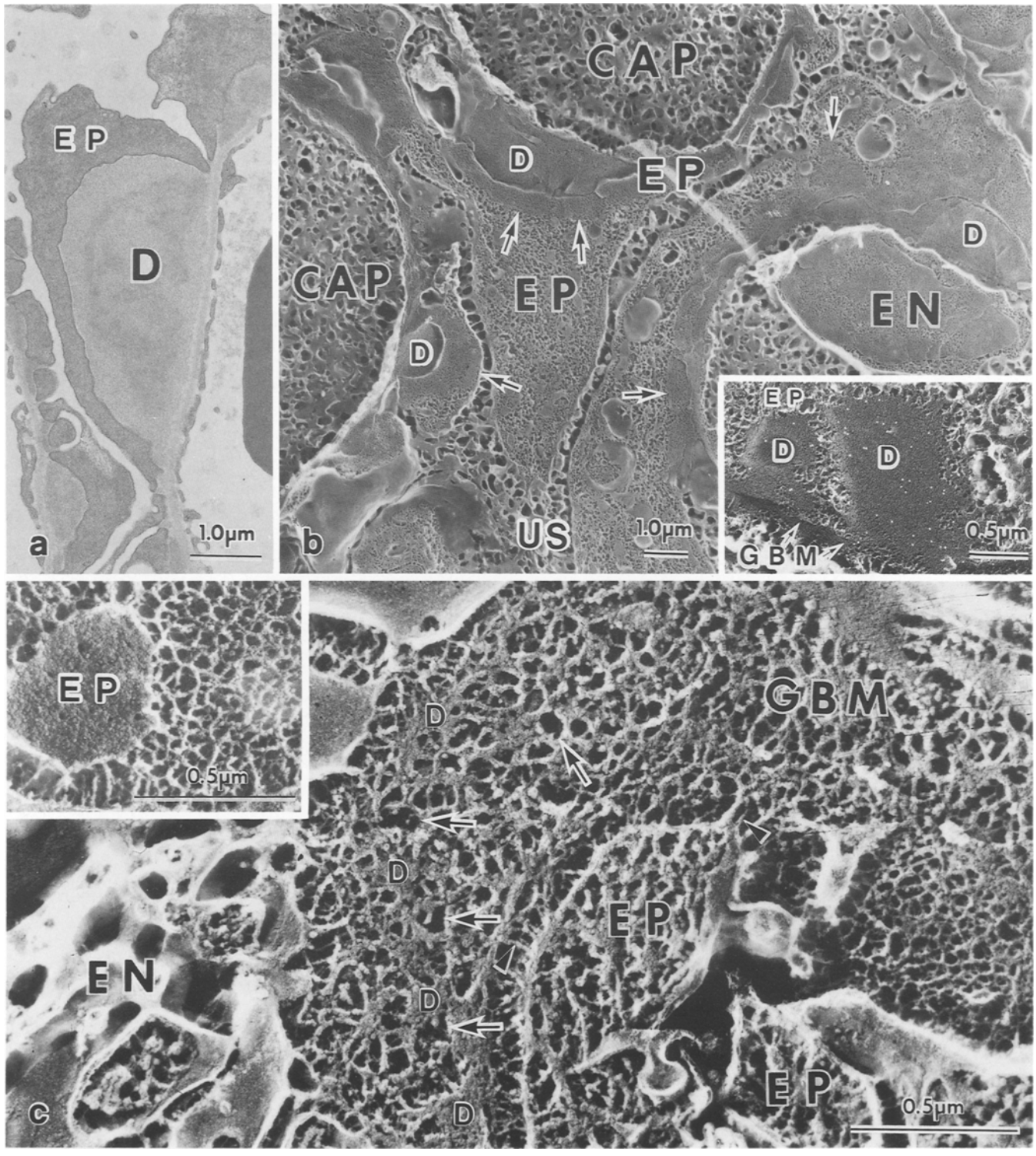

Fig. 2. **a** Electron micrograph of peripheral glomerular basement membrane and podocyte (*EP*) in serum sickness nephritis. *D*, Deposit. ×12000. **b** Replica electron micrograph of peripheral glomerular basement membranes and podocytes (*EP*) in serum sickness nephritis. Hump-like immune deposits (*D*) are localized on the basement membranes. These deposits are covered with densely packed microfilament layers (*arrows*) in the flattened foot processes. *CAP*, Capillary space; *EN*, endothelial cell; *US*, urinary space. ×7200. *Inset*: Anti-IgG localization on replica membrane by freeze-fracture immunohistochemistry. Hump-like granular deposits (*D*) are labelled by 20 nm immunogold. *GBM*, Glomerular basement membrane; *EP*, podocyte. ×19500. **c** Higher magnified replica electron micrograph of immune deposits (*D*) on the lamina densa of glomerular basement membranes (*GBM*) in serum sickness nephritis. Many fibrils organizing the lamina densa are directly attached to the deposits. Networks of lamina densa become irregular due to the dilatation around the deposits (*arrows*), as compared with the regular networks of lamina densa in control rats. (*Inset*: *EP*, Epithelial cell membrane. ×56000.) Connecting fibrils in lamina rara externa are still preserved (*arrowheads*). *EP*, Podocyte; *EN*, endothelial cell. ×56000

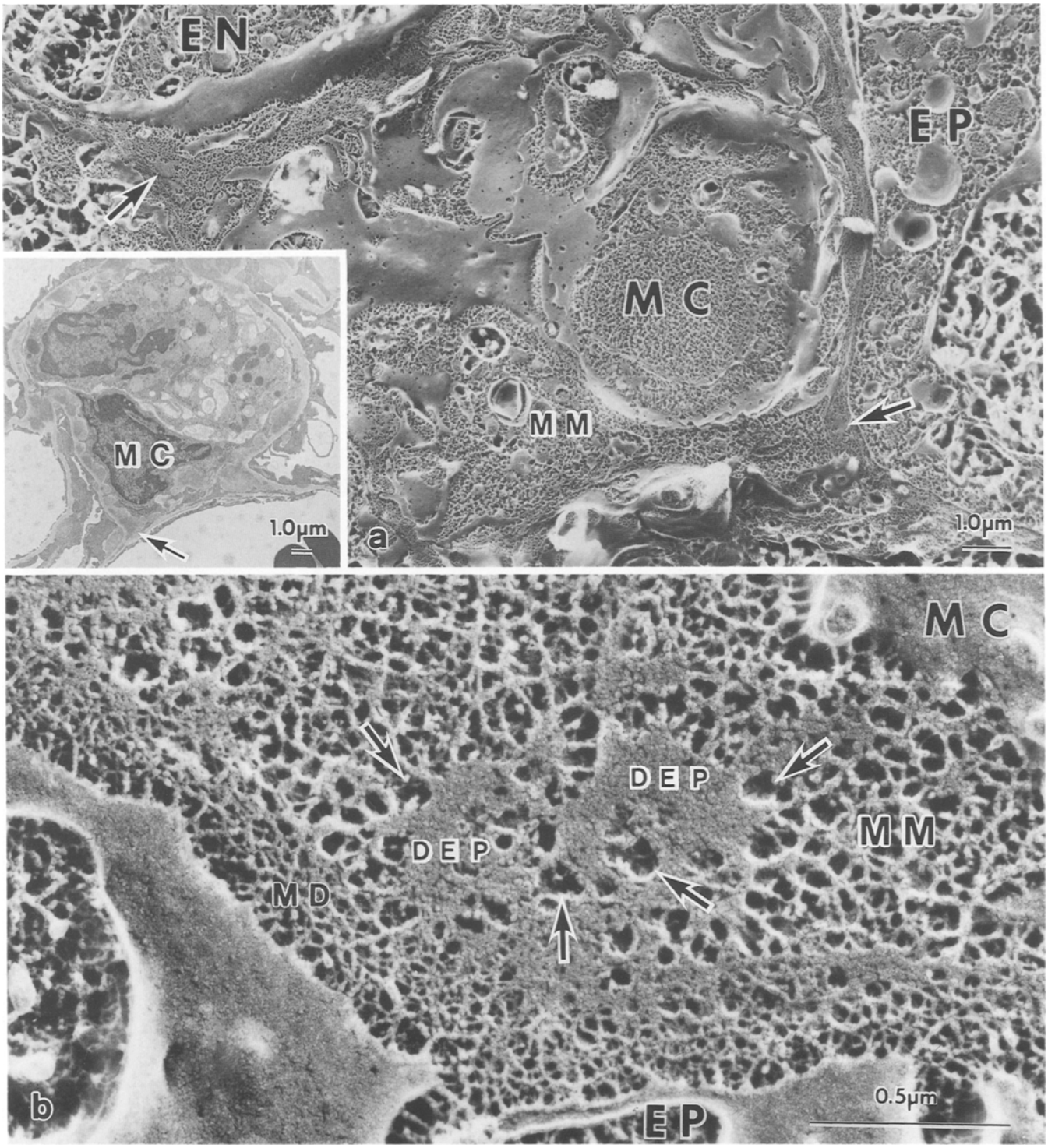

Fig. 3. a Replica electron micrograph of mesangium in serum sickness nephritis. *Arrows* indicate the immune deposits in mesangial angles. *MM*, Mesangial matrix; *MC*, mesangial cell; *EP*, podocyte; *EN*, endothelial cell. ×8400. *Inset*: Corresponding micrograph of conventional ultrathin section. *Arrow* indicates the immune deposit. ×3600. **b** Higher magnified view of immune deposits (*DEP*) in paramesangium in serum sickness nephritis. Meshwork-like fibrils of mesangial matrix (*MM*) and mesangial lamina densa (*MD*) are directly attached to the compact granular deposits. The filamentous networks are observed to be dilated around the deposits (*arrows*). *MC*, Mesangial cell; *EP*, podocyte. ×68000

tion implies that immune deposits can destroy the structure of the constituent fibrillar networks, as observed in the present study. It was also reported that larger immune complexes were preferentially precipitated in the mesangial matrices (Elema et al. 1976; Koyama et al. 1978). Thus the mesangial deposits could also destroy the fibrillar networks of mesangial matrices, resulting in increased or reduced mesangial flow.

Podocytes contain three major cytoskeletal elements, microfilaments, intermediate filaments and microtubules

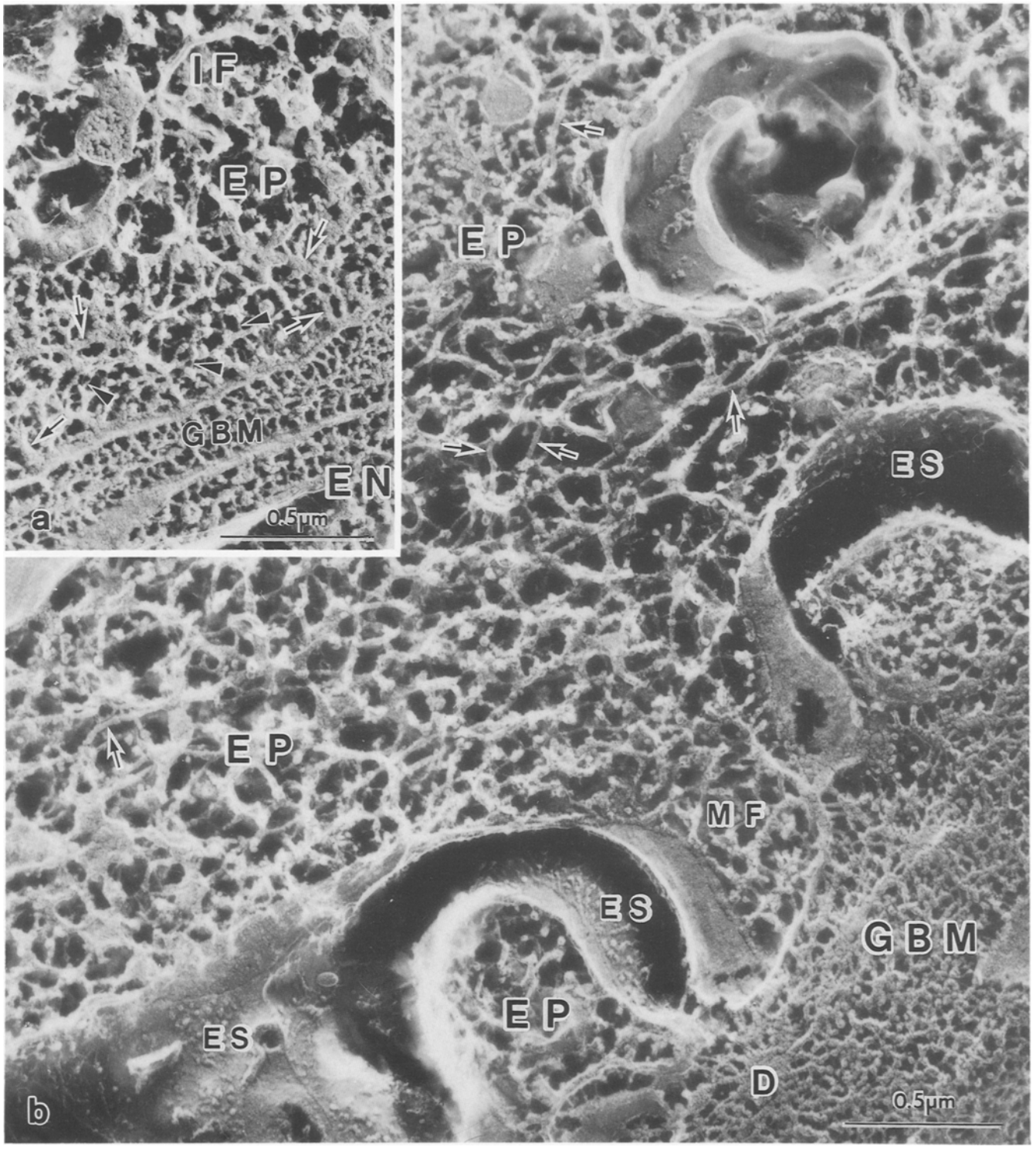

Fig. 4a, b. Replica electron micrograph of S1-treated podocytes in serum sickness nephritis. **a** The S1-decorated actin filaments (*arrows*) are connected with each other and directly attached to the cell membrane beneath the basement membrane (*GBM*), in comparison with undecorated intermediate filaments (*IF*). S1-undecorated fine filaments with diameters of 4–7 nm are connected with actin filaments on their both ends as cross-linking filaments (*arrowheads*). Endothelial cell (*EN*) also contains S1-decorated actin filaments. *EP*, Podocyte. ×52500. **b** Intermediate filaments (*arrows*) are also increased in the primary process of podocytes (*EP*), while S1-decorated actin filaments (*MF*) are increased in the foot process. Glycocalyces are also present on extracellular true surfaces of podocytes (*ES*). *GBM*, Glomerular basement membrane; D, deposit. ×54000

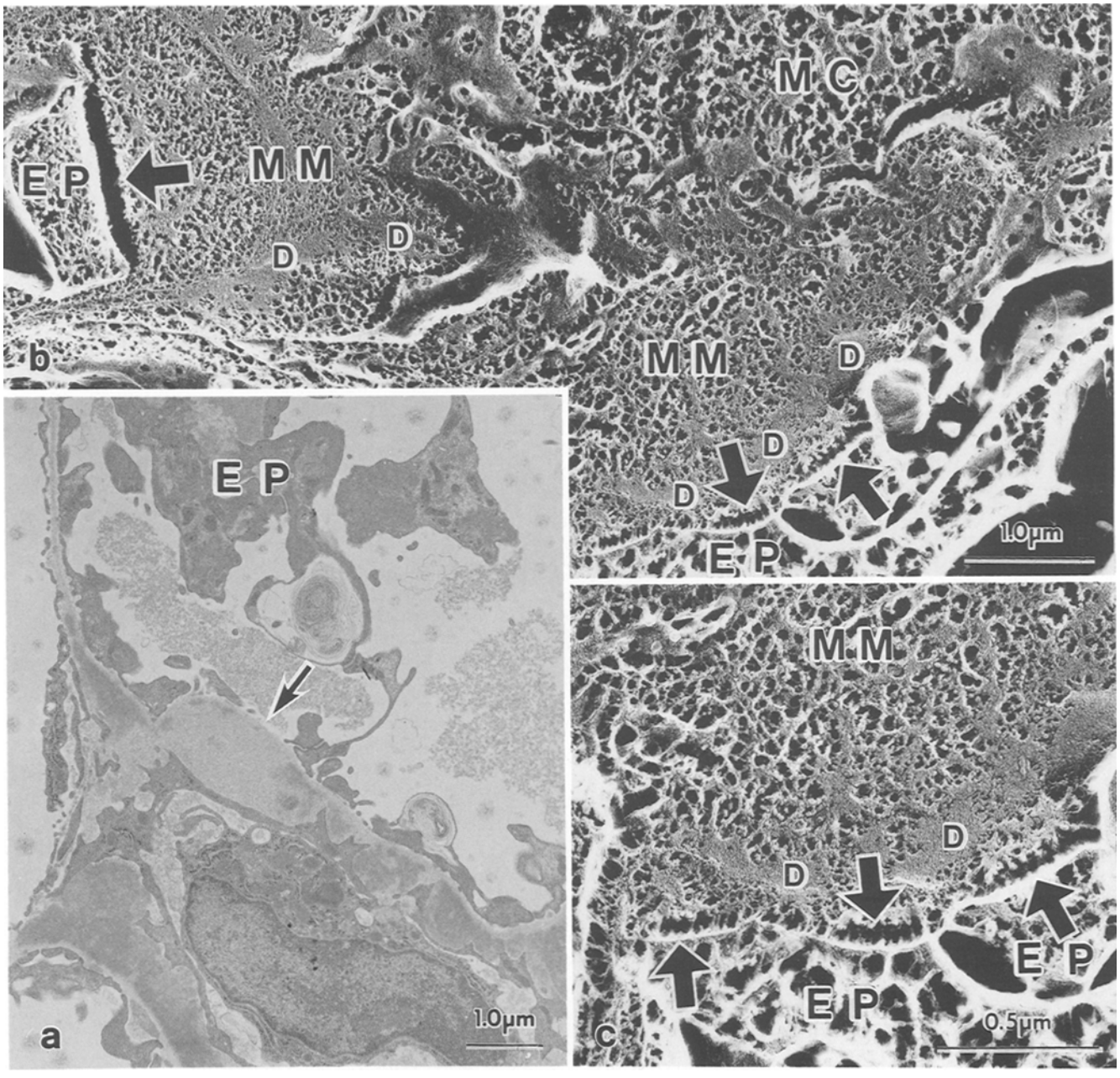

Fig. 5. **a** Conventional electron micrograph of the detachment of podocytes (*arrows*) in serum sickness nephritis. *EP*, Podocyte. ×12000. **b** Replica electron micrograph of initiative change in the detachment of podocytes in serum sickness nephritis. Connecting fibrils in the lamina rara externa are disrupted (*arrows*). *EP*, Podocyte; *MM*, mesangial matrix; *MC*, mesangial cell; *D*, deposits. ×20400. **c** Higher magnified replica electron micrograph of the detachment of podocytes. *Arrows* indicate the disruption of connecting fibrils in the lamina rara externa. *MM*, Mesangial matrix; *D*, deposits; *EP*, podocytes. ×50000

(Vasmant et al. 1984). Drenkhahn and Franke (1988) postulated regional differences in cytoskeletal organization using post-embedding immunoelectron microscopy. Actin proteins were localized in the foot processes and under the cell membranes of cell bodies. However, vimentin and tubulin, the units of intermediate filaments and microtubules respectively, were localized in the cell bodies and their major processes. In our experiments, S1-decorated actin filaments increased in the flattened foot processes and intermediate filaments increased in the cell bodies and their primary processes. Increased intermediate filaments probably work to maintain the structural integrity of podocytes in pathological conditions (Drenckhahn and Franke 1988). We also found S1-undecorated fine filaments between the actin filaments in the flattened foot processes. Recently, six proteins of fine filaments with diameters of 2–5 nm have been identified as the new cytoskeletal components (Roberts 1987). It has been proposed that their function contributes to cell mobility and cytoarchitecture. Drenckhahn and Franke (1988) demonstrated myosin and α-actinin in foot processes, but myosin filaments in

non-muscle cells are too thin to be identified between the bundles of actin filaments (Drenckhahn and Franke 1988; Groschel-Stewart and Drenckhahn 1982). Nevertheless, α-actinin between actin filaments plays a role in generating filaments of opposite polarities. Immunohistochemical methods on replica membranes will be necessary to identify myosin or α-actinin.

The detachment of podocytes from glomerular basement membranes is a serious tissue injury in relation to increasing proteinuria. Focal detachment is known to enhance the permeability of glomerular basement membranes and large molecular proteins could escape into the Bowman's space (Kanwar and Rosenzweig 1982; Whiteside et al. 1989). Moreover, the detachment of podocytes is known to correlate with the development of focal glomerular sclerosis (Kanwar and Farquhar 1980). In our experiment, the detachment was only seen partially and the connecting fibrils in lamina rara externa were disrupted focally in such areas. This finding may represent the initiation stage of detachment of podocytes. It was reported that negative charges in lamina rara externa were important for the attachment of podocytes to glomerular basement membranes (Kihara et al. 1990). In fact, anti-heparan sulphate proteoglycan antibodies could not bind with the areas of subepithelial immune deposition. Actin filaments in the foot processes might be connected with the connecting fibrils in lamina rara externa via the binding proteins, which are vinculin, talin, integrin and fibronectin-laminin receptors (Drenckhahn and Franke 1988). Therefore, we speculate that the increased actin filaments reinforce the connecting fibrils to prevent the detachment of podocytes from the basement membranes.

References

Bolton WK, Sturgill BC (1978) Bovine serum albumin chronic serum sickness nephropathy. Br J Exp Pathol 59:167–177

Dixon FJ, Wilson CB (1976) Recent advances in immunology of glomerulonephritis. In: Giovannetti S, Bonomini V, D'Amino G (eds) Proceedings of the 6th International Congress of Nephrology. Karger, Basel, p 66

Drenckhahn D, Franke RP (1988) Ultrastructural organization of contractile and cytoskeletal proteins in glomerular podocytes of chicken, rat and man. Lab Invest 59:673–682

Elema JD, Hoyer JR, Vernier RL (1976) The glomerular mesangium. Uptake and transport of intravenously injected colloidal carbon in rats. Kidney Int 9:395–406

Groschel-Stewart U, Drenckhahn D (1982) Muscular and cytoplasmic contractile proteins-biochemistry, immunology, structural organization. Coll Relat Res 2:381–463

Heuser H, Kirschner M (1980) Filament organization revealed in platinum replicas of freeze-dried cytoskeleton. J Cell Biol 86:212–234

Kanwar YS, Farquhar MG (1980) Detachment of endothelium and epithelium from the glomerular basement membrane by kidney perfusion with neuramidase. Lab Invest 42:375–384

Kanwar YS, Rosenzweig LG (1982) Altered glomerular permeability as a result of focal detachment of the visceral epithelium. Kidney Int 21:565–574

Kihara I, Kawasaki K, Yaoita E, Yamamoto T (1990) Postembedding immunoelectron microscopic localization of antibodies and complements in the rat with anti-GBM nephritis. Am J Pathol (in press)

Koyama A, Niwa Y, Shigematsu H (1978) Studies on passive serum sickness. II. Factors determining the localization on antigen-antibody complexes in the murine renal glomerulus. Lab Invest 41:253–362

Kubosawa H, Kondo Y (1985) Ultrastructural organization of the glomerular basement membrane as revealed by a deep-etch replica method. Cell Tissue Res 242:33–39

Laurie GW, Leblond CP, Inoue S, Martin GR, Chung A (1984) Fine structure of the basement membrane and immunolocalization of five basement membrane components to the lamina densa (basal lamina) and its extensions in both glomeruli and tubules of the rat kidney. Am J Anat 169:463–481

Naramoto A (1988) Three dimensional examination on the hepatocyte cytoskeleton of phalloidin-treated rats by the quick-freezing and deep-etching replica method. Acta Hepatol Jpn 29:365–376

Naramoto A, Furuta K, Ohno S (1988a) Cytoskeletal organization in the hepatocytes of cholestatic liver models by quick-freezing and deep-etching method. J Clin Electron Microsc 21:708–709

Naramoto A, Nakano M, Itoh N (1988b) Three dimensional examination on the hepatocyte cytoskeleton of obstructive jaundice liver by quick-freezing and deep-etching method. Acta Hepatol Jpn 29:927–937

Naramoto A, Ohno S, Itoh N, Takami H, Nakazawa K, Shigematsu H (1990) Three-dimensional identification of actin filaments in phalloidin-treated rat livers by quick-freezing and deep-etching method. Virchows Arch [A] 417:15–20

Ohno S (1985) Immunocytochemical study on the cytoplasmic side of cell membranes infected with vesicular stomatitis virus by quick-freezing and deep-etching replica method. Histochemistry 82:565–575

Ohno S, Fujii Y (1990) Three-dimensional and histochemical studies of peroxisomes in cultured hepatocytes by quick-freezing and deep-etching method. Histochem J 22:143–154

Ohno S, Takasu N (1989) Three-dimensional studies of cytoskeletal organizations in cultured thyroid cells by quick-freezing and deep-etching method. J Electron Microsc 38:352–362

Roberts T (1987) Fine (2–5 nm) filaments: new types of cytoskeletal structures. Cell Motil Cytoskeleton 8:130–142

Shigematsu H, Yano A (1986) Participation of antigen presenting cells in glomerulonephritis. Acta Pathol Jpn 36:489–497

Vasmant D, Maurice M, Feldmann G (1984) Cytoskeleton ultrastructure of podocytes and glomerular endothelial cells in man and in the rat. Anat Rec 210:17–24

Whiteside C, Prutis K, Cameron R, Thompson J (1989) Glomerular epithelial detachment, not reduced charge density, correlates with proteinuria in adriamycin and puromycin nephrosis. Lab Invest 61:650–660

Yamamoto T, Kihara I, Morita T, Oite T (1978) Bovine serum albumin (BSA) nephritis in rats. I. Experimental model. Acta Pathol Jpn 28:859–866